Cavitation Flow in Nozzle of Liquid Injector

Akira Sou*, Raditya Hendra Pratama, Tsuyoshi Tomisaka, Yusuke Kibayashi
Kobe University, Japan
sou@maritime.kobe-u.ac.jp

Abstract

The cavitation flow in liquid injector nozzles plays an important role in the characteristics of liquid spray. In order to acquire knowledge to predict and control cavitation, this study investigates the effects of an asymmetric inflow from the upstream of the nozzle, needle lift Z, nozzle angle θ, and liquid property by carrying out a visualization of cavitation in two-dimensional nozzles with various Z, θ, and water temperatures T_L. As a result, we found that (1) cavitation occurs and grows asymmetrically in nozzles with an asymmetric inflow, which induces an asymmetric liquid jet behavior, (2) small needle lift increases the thickness of the separated boundary layer and that of asymmetric cavitation, which promote cavitation as well as an asymmetric deformation of a discharged liquid jet, (3) an acute angle of a nozzle inlet promotes cavitation along the acute side of the nozzle wall, (4) inception and development of cavitation in asymmetric nozzles with various needle lifts Z can be predicted quantitatively using the modified cavitation number σ_C, which is based on local pressure at vena contracta, and (5) cavitation length L_{cav} is predictable not by the Reynolds number Re but by the modified cavitation number σ_C.

Introduction

An optimal control of the fuel spray characteristics enables us to improve thermal efficiency and to reduce exhaust gas emissions of internal combustion engines. Since cavitation flow in a nozzle of fuel injectors plays a dominant role in fuel spray characteristics, a large effort has been paid to understand cavitation in single hole nozzles with a symmetric inflow from upstream [1]-[10]. Our knowledge on complex cavitation phenomena in real liquid injectors, such as sac-type nozzles and Valve-Covered Orifice (VCO) nozzles, into which liquid fuel flows asymmetrically, is not sufficient [11]-[15]. Cavitation in a nozzle is affected by liquid velocity, geometry of the injector, needle lift, length-to-diameter ratio of the nozzle, curvature of the inlet edge, liquid property, dissolved gases in a liquid, system pressure, and so on. In this study we focus on the effects of an asymmetric inflow, needle lift and liquid property on cavitation, and a discharged liquid jet near the nozzle. Cavitating water flows in various two-dimensional nozzles with different needle lifts Z and water temperatures T_L are visualized using a digital camera and high-speed cameras. The length L_{cav} and profiles $y_{cav}(x)$ of the cavitation zone are measured for various liquid velocities V to investigate the relationship between the flow contraction at the nozzle inlet, cavitation behavior, and liquid jet deformation. The Reynolds number Re and some cavitation numbers have been widely used as dominant parameters for cavitation flow in a nozzle. The applicability of the modified cavitation number σ_C [7], [9] to the cavitation in the nozzles is also examined.

Effects of Asymmetric Inflow on Cavitation and Jet

Figure 1 (a) and (b) illustrate a sac-type injector used for low-speed marine diesel engines and a Valve Covered Orifice (VCO) nozzle, respectively. One of the dominant features of the internal flow in these real nozzles is the asymmetric inflow. In this study cavitation in nozzles with an asymmetric inflow is investigated.

Figure 2 shows the schematic of experimental setup. Filtered tap water is injected into ambient air through various transparent nozzles with an asymmetric inflow. The details of the experimental setup can be found in Ref. [6]. Still images of cavitation in the nozzles are captured using a digital camera (Fujifilm, FinePix S3Pro, 4256 x 2848 pixels) and a flush lump (Nisshindenki Co., Micro Flash Stroboscope, MS-1000/LH-15M, duration 4 μs). High-speed images of the cavitation and the jets are takes by high-speed cameras (Photron, FASTCAM SA5 and SA-X) and a metal-halide lamp (Kyowa Co. Ltd., MID-25FC).

As shown in Figs. 3(a) and (b), two-dimensional nozzles consisting of two acrylic flat plates and two stainless steel thin flat plates, by which sharp-edges were formed at the inlet of the nozzle, were used to measure and quantitatively evaluate the cavitation. Asymmetric nozzles illustrated in Fig. 3(b) are manufactured to investigate the effects of an asymmetric inflow on cavitation and the jets. The geometry of the 2D nozzles represents the flow channel indicated by the tetragons in Figs. 1(a) and (b). The width W, length L and thickness t of the nozzles were 4 mm, 16 mm, and 1 mm, respectively. Asymmetric nozzles with different needle lifts Z of 4, 8, and 16 mm (Z/W = 1, 2 and 4) were used to examine the effects of needle lift on cavitation and the jets.

Nozzles with various nozzle angles θ (θ = -30, -20, 0, 20, 30 deg.), which is defined in Fig. 4, were used to investigate the effects of nozzle angle on cavitation and the discharged liquid jets.

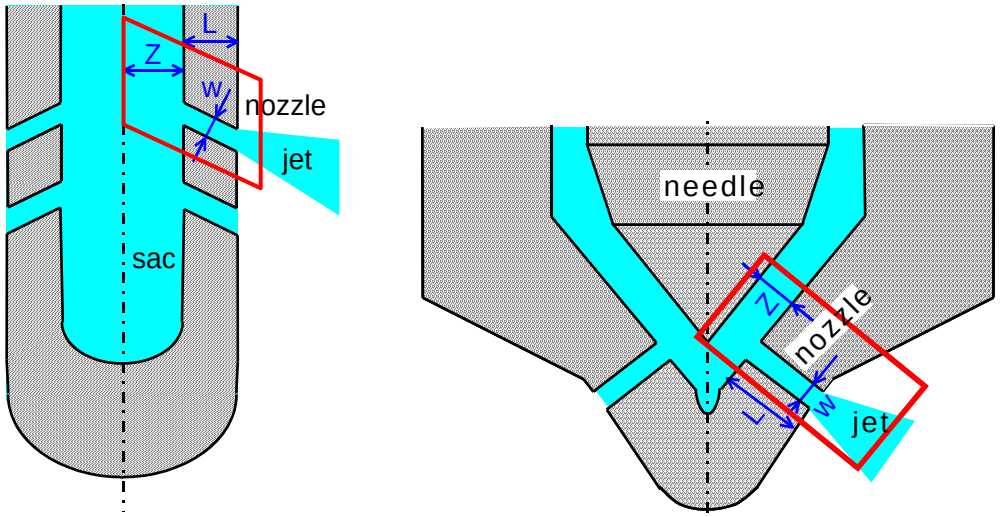

(a) sac-type injector (b) Valve Covered Orifice (VCO) nozzle

Figure 1 Sac-type injector and Valve Covered Orifice (VCO) nozzle.

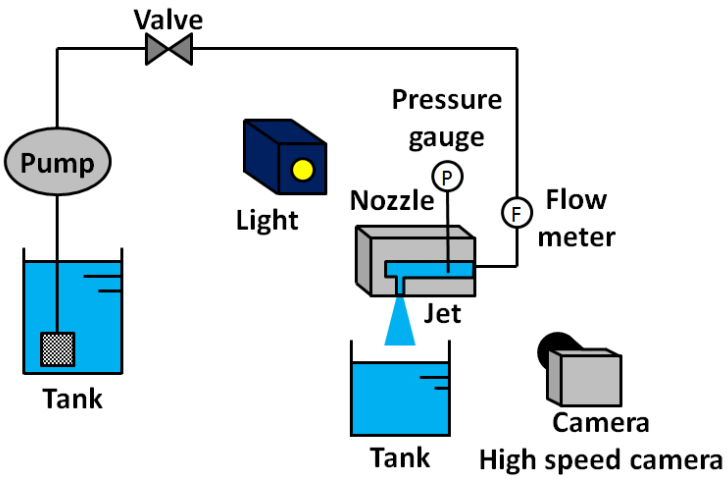

Figure 2 Schematic of experimental setup.

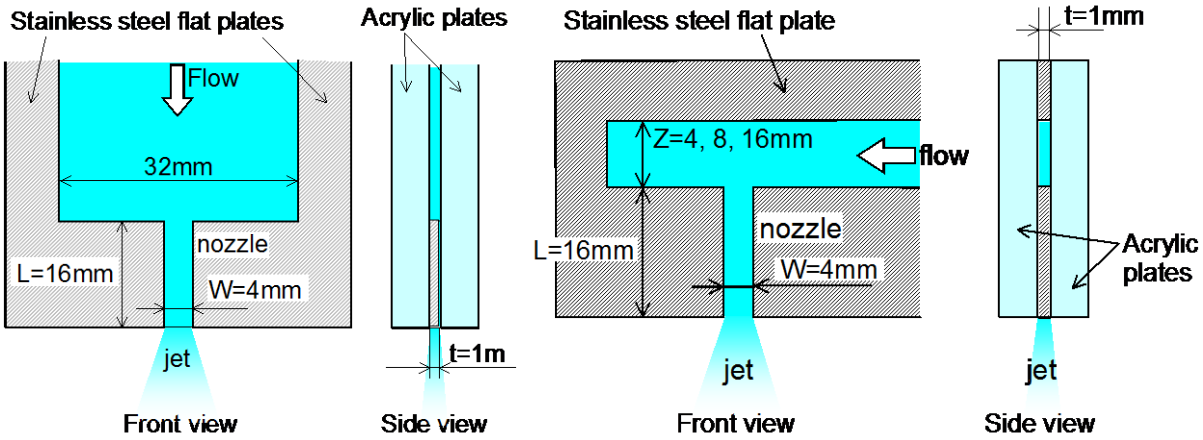

(a) symmetric nozzle (b) nozzles with an asymmetric inflow

Figure 3 Schematics of two-dimensional nozzles.

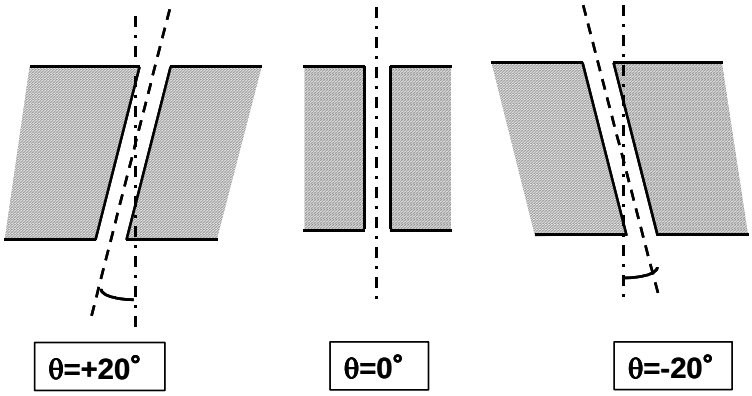

Figure 4 Schematics of two-dimensional nozzles with different angles θ.

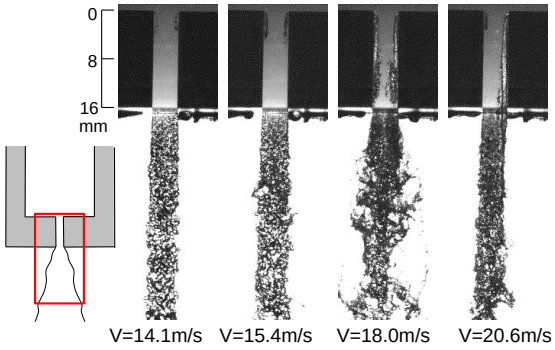

(a) symmetric nozzle

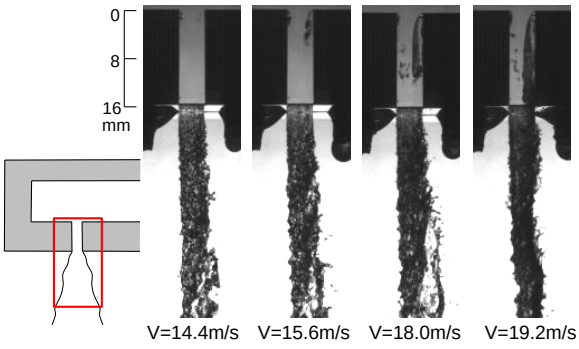

(b) asymmetric nozzle, Z/W=4, θ=0 degree

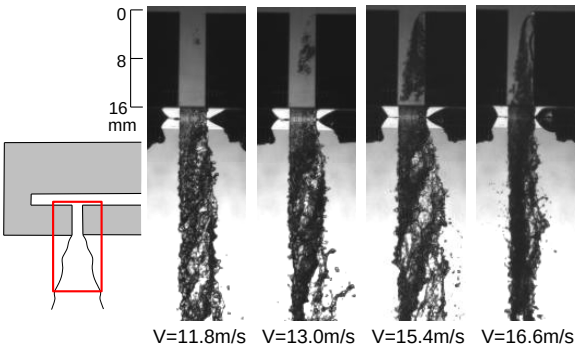

(c) asymmetric nozzle, Z/W=1, θ=0 degree

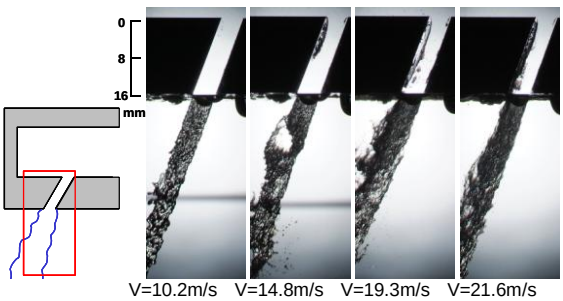

(d) asymmetric nozzle, Z/W=4, θ=20 degree

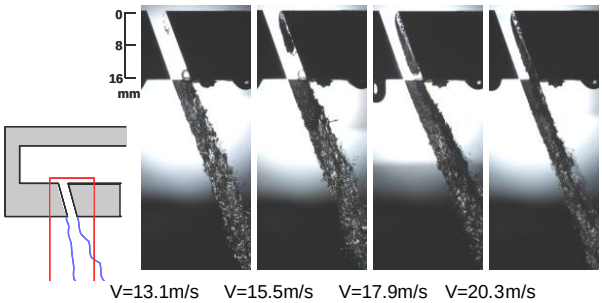

(e) asymmetric nozzle, Z/W=4, θ= –20 degree

Figure 5 Cavitation in nozzles and liquid jets.

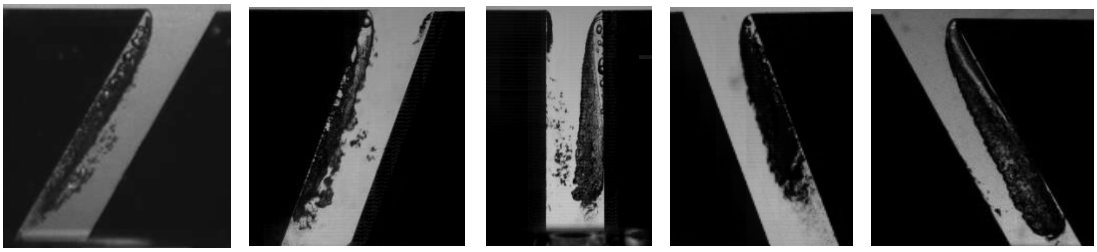

(a) θ = 30 deg (b) θ = 20 deg. (c) θ = 0 deg. (d) θ = -20 deg. (e) θ = -30 deg.

Figure 6 Cavitation in various tilted nozzles.

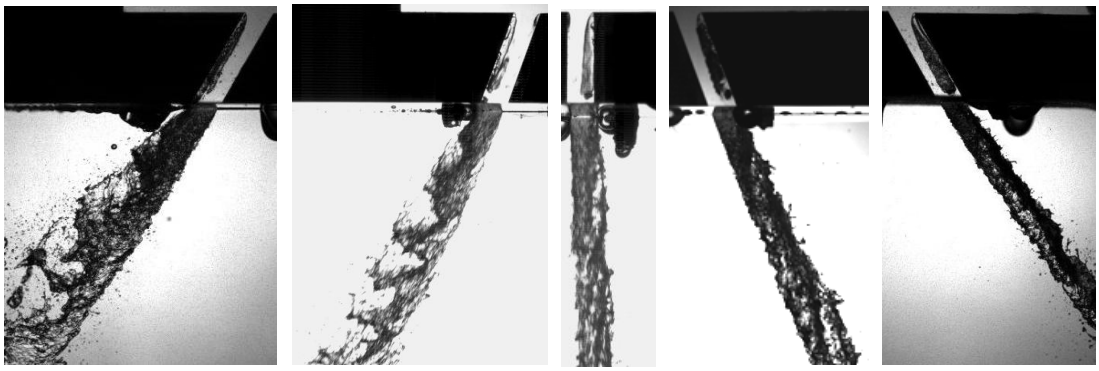

(a) θ = 30 deg (b) θ = 20 deg. (c) θ = 0 deg. (d) θ = -20 deg. (e) θ = -30 deg.

Figure 7 Cavitation in various tilted nozzles and liquid jets.

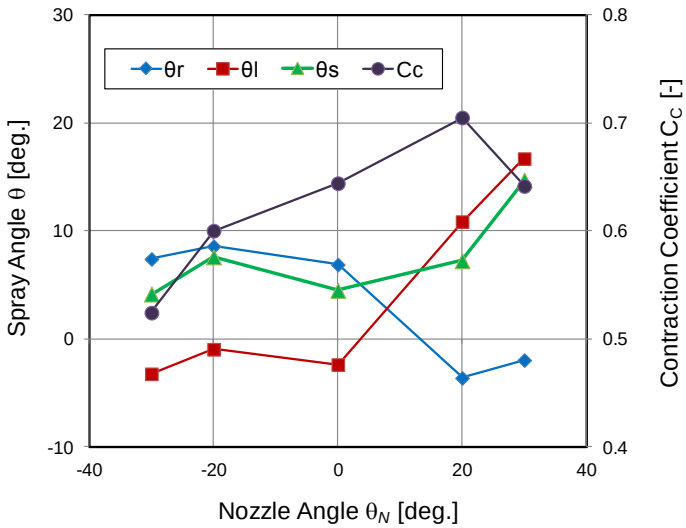

Figure 8 Effects of nozzle angle on contraction coefficient and jet angle.

Figure 5 shows the photos of cavitation in the nozzles and the injected liquid jets near the exit. Figure 5(a) represents the case of the symmetric nozzle. As reported in Ref. [6], inception and development of cavitation appear almost symmetrically. Cavitation occurs along the outer edge of the separated boundary layer near the inlet, grows symmetrical almost to the exit (supercavitation [4]), and finally becomes a hydraulic flip [6], [11]. In supercavitation a liquid jet is deformed drastically by cavitation, and injection angle θ_s of the discharged liquid jet increases [3], [6].

As shown in Figs. 5(b) and (c), in the asymmetric nozzles cavitation appears and grows mainly along the upstream (right) side of the nozzles, and the upstream (right) side of the liquid jet deforms largely due to the asymmetric cavitation. We found clear evidence that the decrease in needle lift *Z* results in a larger deformation of liquid jet and a larger injection angle.

Figures 5(d), 5(e), 6 and 7 show cavitation in the inclined nozzles and the jets. Cavitation does not always occur along the upstream (right) side but along the side of an acute angle, where a separated boundary layer is thicker. As shown in Fig. 8, an acute nozzle angle θ increases cavitation thickness and hence decreases the

contraction coefficient C_C. Right (r), left (l) and total (s) angles θ of the discharged liquid jet measured at 32 mm downstream of the exit are shown in Fig. 8. These results imply that the acute angle of the inlet edge promotes the asymmetric cavitation and asymmetric jet deformation.

Figure 9 shows the thickness y_{cav} of cavitation normalized by nozzle width W. The cavitation profiles indicate that cavitation thickness y_{cav} increases with decreasing needle lift Z. Consequently, as shown in Fig. 10, the ratio between the width of the core flow W_L and that of nozzle W, *i.e.*, contraction coefficient C_C, decreases with decreasing Z. These trends suggest that although a small needle lift tends to reduce liquid flow rate in VCO nozzles, it increases the thickness of the separated boundary layer, and might promote cavitation. The expectation agrees with the relations between measured cavitation length L_{cav} and liquid velocity V shown in Fig. 11(a) for various needle lifts Z. In other words, cavitation takes place and develops at lower velocity in the case of smaller needle lift. Figure 11(a) implies that inception and development of cavitation occur at different V for the nozzles with different Z. One of the authors has reported that the modified cavitation number σ_C enables us to quantitatively predict cavitation in nozzles with different upstream cross-sectional areas [7] and different length-to-diameter ratios [9]. The σ_C is based on the local pressure at the vena contracta and takes into account the flow contraction in a nozzle, and is defined by [7]

$$\sigma_C = C_C^2 \left[\frac{P_b - P_v}{\frac{1}{2}\rho V^2} + \frac{\lambda L}{D_H} + 1 \right] \tag{1}$$

where P_b is the back pressure, P_v the vapor saturation pressure, ρ the liquid density, λ the friction factor, D_H the hydraulic diameter, respectively.

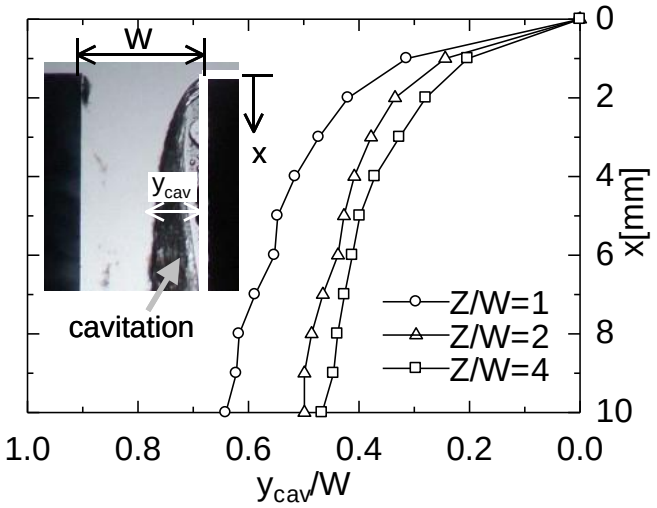

Figure 9 Effect of needle lift Z on cavitation thickness y_{cav}.

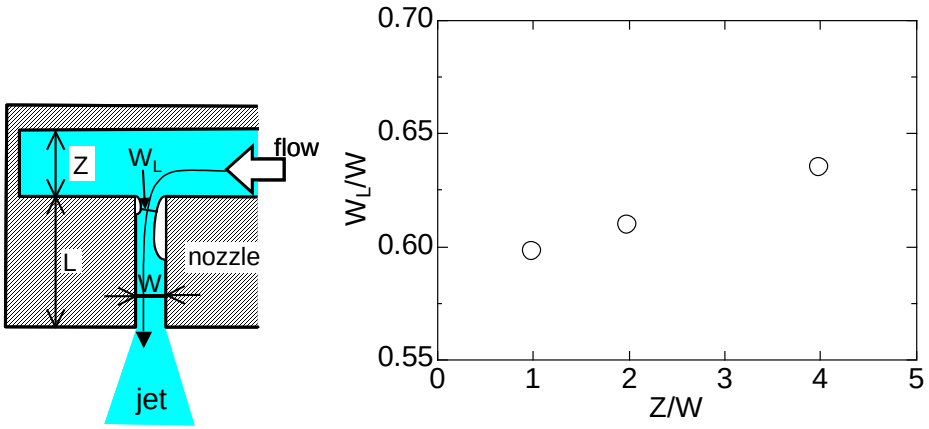

Figure 10 Effect of needle lift Z on contraction coefficient W_L/W (=C_C).

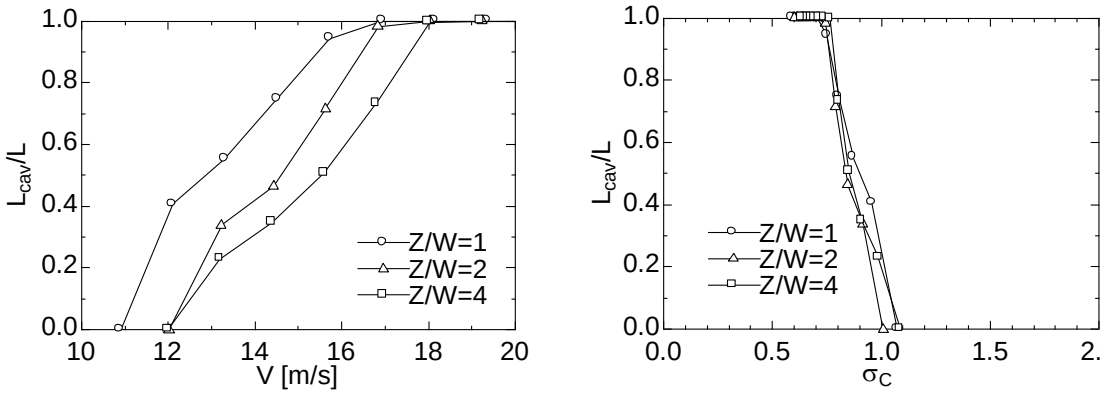

(a) L_{cav}/L vs. V (b) L_{cav}/L vs. σ_C

Figure 11 Effect of needle lift Z on cavitation length L_{cav}.

As shown in Fig. 11(b), the relation between normalized cavitation length L_{cav}/L and the modified cavitation number σ_C confirms that the inception and development of cavitation in asymmetric nozzles with different needle lifts Z can be quantitatively estimated by using σ_C, i.e. by knowing the local pressure at vena contracta.

Figures 12 shows the high-speed image of cavitation in the nozzle with small lift (Z/W = 1, V = 13.0 m/s) and θ = 0 degree, as well as the injected jet. When a large cloud of cavitation or a large vortex remaining after the collapse of the cavitation flows along the right wall out of the nozzle, the right part of the liquid jet deforms drastically and asymmetrically. A similar phenomenon has been observed in a symmetric nozzle [6]. Since the separated boundary layer and cavitation zone in the nozzle with an asymmetric inflow are thick and the cavitation clouds are large, the scale of the jet deformation is large.

Figure 13 shows the time history of the tail position of cavitation cloud L_{cloud} and that of the right side angle θ_R of the liquid jet measured at the distance of 16 mm from the exit. The result clearly shows that a semi-periodic cloud-shedding induces a semi-periodic deformation of the right interface with the delay of about 2 ms, which corresponds to the time for the vortex to arrive at the measurement position. The Strouhal number St of the cloud-shedding and jet deformation, which is defined by

$$St = \frac{fL}{V}, \tag{2}$$

is about 0.56. Here f denotes the mean frequencies of cavitation cloud-shedding and liquid jet deformation, L is the nozzle length, and V is the mean liquid velocity in the nozzle, respectively. The value of St is slightly smaller than the case of the symmetric nozzles [6], which is most likely due to the thicker boundary layer and larger vortex.

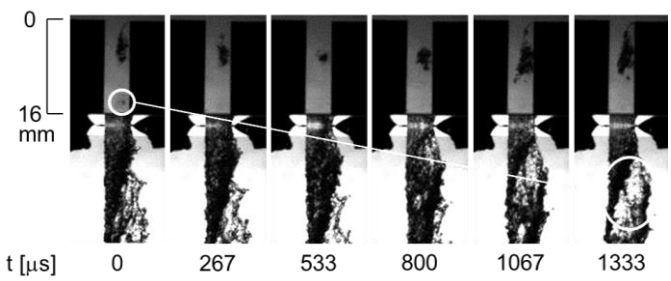

Figure 12 High-speed image of cavitation and a jet (Z/W = 1, V = 13.0 m/s).

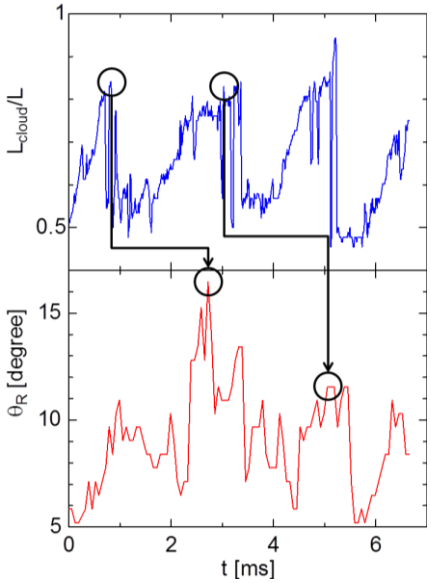

Figure 13 Time histories of the tail position L_{cloud} of cavitation clouds and jet angle θ_R.

Effects of Fluid Property on Cavitation and Jet

Fluid properties play an important role in cavitation and liquid spray. One of the authors has pointed out through the observation of cavitation in water with various temperatures T_L that the cavitation regime can be predicted not by the Reynolds number *Re* but by a cavitation number σ for *Re* > 30000 [6]. Table 1 shows the density ρ, vapor saturation pressure P_v, viscosity μ, and surface tension σ of water with various temperatures T_L. The trends indicate that by changing T_L from 285 K to 326 K we can vary water properties, and thus the Reynolds number *Re* and the modified cavitation number σ_C. Ten photos of cavitation in the symmetric nozzle shown in Fig. 3(a) and the jet were taken using a digital camera for each liquid velocity *V* and water temperature T_L. Volume flow rate was carefully calibrated for each water temperature T_L. The maximum error of measured flow rate was 3.0 %.

Table 1 Property of water.

Temperature T_L [K]	285	305	326
Density ρ [kg/m^3]	999	995	987
Vapor saturation pressure P_v [kPa]	1.4	4.7	14.2
Viscosity μ [mPa.s]	1.24	0.77	0.52
Surface tension σ [mN/m]	74	71	67

Photos of cavitation and jets with various T_L are shown in Fig. 14. Although cavitation and jet regimes at different T_L show the same trends, regime transitions occur at higher *V* in the case of lower T_L. Figure 15 shows measured profile $y_{cav}(x)$ of the cavitation film for each T_L, which is not dependent on T_L in the range of this study (*Re* >12500). The match implies that C_C does not depend on T_L. However, normalized lengths L_{cav}/L of cavitation under the same *V* or the same *Re* are different for different T_L, as is clearly shown in Fig. 16 (a) and (b). On the other hand, cavitation lengths L_{cav}/L at a σ_C show close similarities even for different water temperatures T_L. Since the modified cavitation number σ_C is an index based on local pressure at vena contracta, the agreement indicates that local pressure at vena contracta is the key parameter.

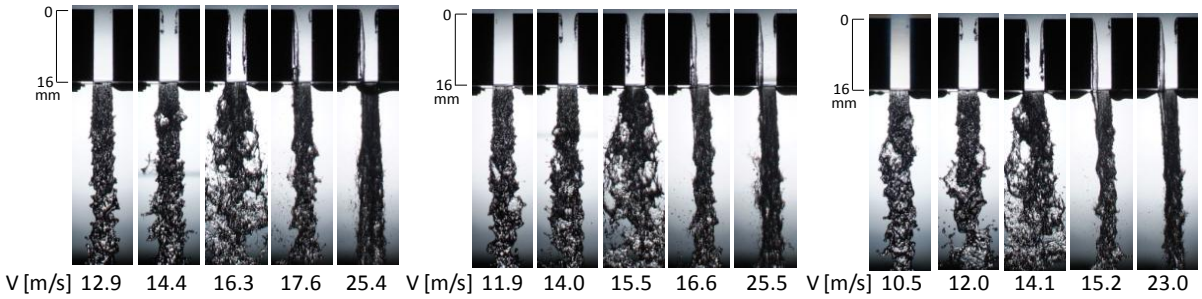

(a) T_L = 285 K (b) T_L = 305 K (c) T_L = 326 K

Figure 14 Cavitation with various water temperatures.

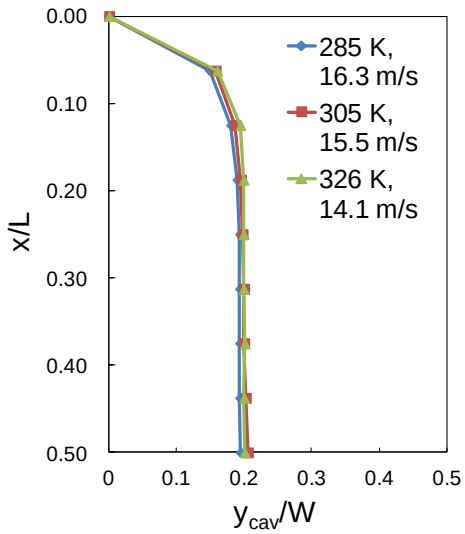

Figure 15 Normalized cavitation profiles y_{cav} along the streamwise axis *x* for various liquid temperatures T_L.

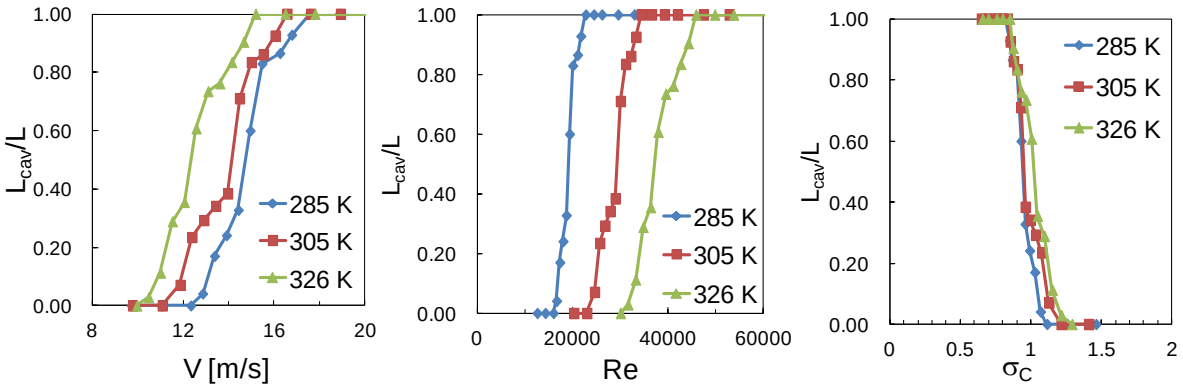

(a) L_{cav}/L vs. V (b) L_{cav}/L vs. Re (c) L_{cav}/L vs. σ_C

Figure 16 Relations between cavitation length L_{cav} and dimensionless numbers Re, σ_C.

Conclusions

Cavitation in a symmetric nozzle and some nozzles with an asymmetric inflow for variations of needle lifts Z, nozzle angles θ, and water temperatures T_L was captured using a digital camera and high-speed cameras for investigation in this study. As a result, we obtained the following conclusions:

(1) Cavitation occurs and grows asymmetrically in asymmetric nozzles, which finally induces an asymmetric liquid jet deformation.

(2) Small needle lift increases the thickness of the separated boundary layer and cavitation film, which promotes the inception and development of cavitation as well as liquid jet deformation.

(3) An acute angle of a nozzle inlet promotes cavitation and a large deformation of discharged liquid jet.

(4) Inception and development of cavitation in asymmetric nozzles with various needle lifts can be predicted quantitatively using the modified cavitation number σ_C, which is based on local pressure at vena contracta.

(5) Cavitation length L_{cav} is predictable not by using the Reynolds number Re for the range of $Re > 12500$, but by the modified cavitation number σ_C.

(6) Cavitation induced by the flow separation in a nozzle of liquid injectors is strongly affected by the profile of the separated boundary layer, which depends not on the Reynolds number Re, but instead strongly on an asymmetric inflow, needle lift Z and nozzle angle θ.

Acknowledgements

This study was partly supported by a Grant-in-Aid for Scientific Research (C) (#20560160) of the Japan Society for the Promotion Science (JSPS). The authors would like to express their thanks to Mr. K. Takayama in Photron ltd. for his support.

References

[1] Bergwerk, W., *Proc. Institute of Mechanical Engineers*, 173-25, pp. 655–660 (1959).
[2] Nurick, W. H., *J. Fluid Engng., Trans. ASME*, pp. 681–687 (1976).
[3] Hiroyasu, H., Arai, M., Shimizu, M., *Proc. ICLASS 91*, pp. 275–282 (1991).
[4] Chaves, H., Knapp, M., Kubitzek, A., Obermeier, F., Schneider, T., *SAE Paper*, Paper No. 950290, pp. 645–657 (1995).
[5] Tamaki, N., Shimizu, M., Nishida, K. and Hiroyasu, H., *Atomization and Sprays*, 8, pp. 179–197 (1998).
[6] Sou, A., Hosokawa, S., Tomiyama, A., *Int. J. Heat and Mass Transfer*, 50, 17-18, pp. 3575–3582 (2007).
[7] Sou, A., Maulana, M.I., Isozaki, K., Hosokawa, S., Tomiyama, A., *J. of Fluid Sci. and Technol.*, 3-5, 622–632 (2008).
[8] Sou, A., Maulana, M.I., Hosokawa, S., Tomiyama, A., *J. of Fluid Sci. and Technol.*, 3-5, 633–644 (2008).
[9] Sou, A., *SAE Int. J. of Engines*, 2-2, pp. 694–702 (2010).
[10] Sou, A. and Kinugasa, T., *Proc. THIESEL 2010*, pp. 53–61 (2010).
[11] Soteriou, C., Andrews R.J., Torres N., Smith M. and Kunkulagunta R., *Proc. ILASS-Europe 2001*, pp. 574–579 (2001).
[12] Ganippa, L.C., Bark, G., Andersson, S., Chomiak, J., *Proc. 4th Int. Symp. on Cavitation*, A9.005 (2001).
[13] Arcoumanis, C., Gavaises, M., Roth, H., Choi, Y.S., Theodorakakos, A., *Proc. THIESEL 2002*, A.1 (2002).
[14] Miranda, R., Chaves,H., Martin, U., Obermeier, F., *Proc. ICLASS 2003*, ICLASS03-1206 (2003).
[15] Payri, F., Bermudez, V., Payri, R., Salvador, F.J., *Fuel*, 83, pp. 419–431 (2004).